

**ONSET OF CHANNEL FLOW REVERSAL
IN RD-14M NATURAL CIRCULATION TESTS**

**P.T. Wan, W.I. Midvidy, J.C. Luxat
Nuclear Safety Department
Ontario Hydro
700 University Avenue
Toronto, Ontario
M5G 1X6**

**A paper presented at the 13th Annual Conference of the Canadian Nuclear Society
Saint John, New Brunswick
June 8-10, 1992**

ONSET OF CHANNEL FLOW REVERSAL IN RD-14M
NATURAL CIRCULATION TESTS

P.T. Wan, W.I. Midvidy and J.C. Luxat
Nuclear Safety Department
Ontario Hydro
700 University Avenue
Toronto, Ontario, M5G 1X6

ABSTRACT

This paper presents an analysis of the conditions leading to the onset of channel flow reversal in a series of natural circulation tests conducted in the RD-14M facility. This series of tests was carried out to investigate two-phase natural circulation under conditions of decreasing primary inventory, but with no break in the heat transport system.

In these tests, the channel flows were found to be unidirectional in the early part of each experiment. Then, depending on the specific test conditions, the flow in some channels reversed, while the flow in the remaining channels continued in the same direction.

A conceptually simple flow-reversal criterion is applied to these tests: the prevailing header-to-header pressure differential (ΔP_{HH}) must be sufficiently negative to overcome the forward driving force resulting from the density gradient between the inlet and outlet feeders. A comparison between the predictions using the above criterion and the experimental data is made in the following areas:

- (1) the magnitude of the ΔP_{HH} at the onset of channel flow reversal, and
- (2) which of the channels is the first to reverse.

For those tests which exhibited relatively steady ΔP_{HH} , the ΔP_{HH} was observed to become increasingly negative as the loop liquid inventory was reduced. The mechanism responsible for the increasingly negative ΔP_{HH} is described. Using the above flow-reversal criterion, the header-to-header pressure differential required for the onset of channel flow reversal, ΔP_{rev} , is computed using experimental values as a function of time. Onset of channel flow reversal is observed to occur when the absolute magnitude of the experimentally measured ΔP_{HH} exceeds that of ΔP_{rev} . Furthermore, the criterion predicts the top channels to be the first to reverse in these tests, which is in agreement with the experimental results for the tests which exhibited steady flow.

For those tests which exhibited oscillatory ΔP_{HH} , the amplitude of the oscillations was observed to increase as the loop liquid inventory was reduced. A qualitative explanation for the

oscillatory behaviour of the loop is given. Using the above flow-reversal criterion, the header-to-header pressure differential required for the onset of channel flow reversal, ΔP_{rev} , is computed as a function of time. When the experimentally measured ΔP_{HH} approaches ΔP_{rev} , temporary flow slowdowns are observed. When the absolute magnitude of the experimentally measured ΔP_{HH} significantly exceeds that of ΔP_{rev} , onset of sustained channel flow reversal is observed. Applying the above criterion to these tests, it is shown that the top channels are not necessarily the first to reverse. However, the above flow-reversal criterion is unable to predict which of the channels is the first to reverse in these tests. Development of a dynamic flow-reversal criterion, accounting for the transient and feedback processes occurring in these tests, is in progress.

A model of the below-header components in the RD-14M loop is under development. The model has been used to predict the fluctuation in ΔP_{HH} required for channel flow reversal as a function of the average ΔP_{HH} . The model also predicts that smaller fluctuations in ΔP_{HH} are sufficient for reversal of the channel flow when the net channel power is decreased. It is planned to integrate the present "below-header" model with an "above-header" model to predict the primary inventory at the onset of channel flow reversal. When an integrated model is developed, the effect of heat losses on the primary inventory at the onset of channel flow reversal will be determined.

The experiments described in this paper were performed by Whiteshell Laboratories of AECL Research, and funding for these experiments was provided by the CANDU Owners Group. The analysis described in this paper was performed by Ontario Hydro.

INTRODUCTION

RD-14M (Figure 1) is a multiple-channel pressurized-water test facility with its components arranged in a figure-of-eight heat transport circuit. For a detailed description of the experimental facility, the interested reader is referred to reference 1.

The T88-series of experiments was carried out to investigate two-phase natural circulation flow in the RD-14M facility. Each experiment was started with the loop in single-phase thermosiphoning conditions. By controlled intermittent draining of the liquid inventory from the loop, two-phase natural circulation was established. It should be noted that there was no "real" break in the heat transport system in these tests. The intention was to minimize the effect of draining on the results. The system parameters were then allowed to stabilize before the next draining. Intermittent draining of the loop inventory continued until a process protection trip (usually high sheath temperature of $\sim 600^{\circ}\text{C}$) occurred, thus terminating the experiment.

In the figures in this paper, small arrows are used to denote the beginning and end of each drain, while large arrows are used to denote the occurrence of channel flow reversals. Furthermore, a 9-point (18-second) averaging scheme has been used to smooth out some of the fluctuations in the following figures. Some of the fluctuations that occurred in the measurements of these thermosiphoning tests may be attributed to instruments recording at levels that were considerably less than 25 percent of full scale.

In these tests, the channel flows were found to be unidirectional in the early part of each experiment. Then, depending on the specific test conditions, the flow in some channels reversed, while the flow in the remaining channels continued in the same direction. The results of this series of RD-14M tests have been reported and analyzed by various authors [2-7].

The onset of channel flow reversal denotes the establishment of an alternative pathway for the coolant in the heat transport system whereby fluid in the same core pass could be recirculated through the headers without going through the steam generators - the "intended" heat sink. (In these RD-14M tests, there were significant below-header heat losses, which represents a major unintended heat sink.) In every case, the onset of channel flow reversal coincided with a reduction of flow through the steam generators. In some cases, it coincided with a complete cessation of flow through the steam generators. As a result, the fluid temperatures in the inlet and outlet headers (Figure 2) approached a common value, and the density gradient for driving the flow between the inlet and outlet feeders began to diminish. Eventually (usually with further draining), a limiting temperature excursion in excess of 600°C occurred, terminating the experiment.

In the high power (160 kW/pass) tests, the limiting temperature excursions were observed to occur at primary inventories that were slightly less than those required for the onset of channel flow reversal. In medium (100 kW/pass) and low (60 kW/pass) power tests, the limiting temperature excursion was observed to occur at primary inventories that were significantly less than those for the onset of channel flow reversal. A summary of these results can be found in reference 5.

It is known that heat losses from the RD-14M thermosiphoning tests were significant, hence interpretation and extrapolation of these test results to other situations must account for heat loss effects. Figure 3 shows the estimated heat losses from the loop as a function of primary coolant temperature [8].

The present work focuses on the conditions leading to the onset of sustained channel flow reversal in these partial inventory thermosiphoning tests. The present work concentrates on the analysis of high power thermosiphoning tests since the influence

of heat losses on the overall results was relatively smaller other things being equal. A brief summary of the test conditions and results in these high power tests is shown in Table 1.

SYSTEM RESPONSE TO INTERMITTENT DRAINING

Before proceeding to discuss the conditions leading to the onset of channel flow reversal in these (160 kW T88) tests, it is desirable to examine the behaviour of the header-to-header pressure differentials in these tests. In some cases, the header-to-header pressure differentials were relatively steady. In other cases, they were highly oscillatory. These oscillations can be caused by (a) the draining operation, (b) the system conditions following the drain, and (c) a combination of the above two factors (i.e., it may take a draining operation of a certain rate and a certain set of system conditions to produce these oscillations). It is not possible at this time to determine which of the above factors is dominant in these tests.

The stability of two-phase flows in a figure-of-eight configuration has been investigated by many authors [9-12]. Various methods are available for determining the conditions under which oscillations in a figure-of-eight loop occur and the nature of the oscillations. Alternatively, advanced two-fluid thermalhydraulics codes, such as TUF and CATHENA, should also be able to predict the steady and oscillatory characteristics of the loop for various conditions.

Using the spring-mass analogy in reference 10, a simplified description of the mechanism is as follows. Basically, the two-phase region is compressible and acts like a spring. The single-phase liquid region acts like an incompressible mass, giving substantial inertia to the system. During the draining operation, header 7 becomes the lowest pressure point in the RD-14M loop and the void introduced as a result of draining is concentrated in the piping in the vicinity of header 7. This causes the fluid in the upstream pass (channels 5 to 9) to accelerate and the fluid in the downstream pass (channels 10 to 14) to decelerate. After the draining operation has stopped, the inertia of the system causes increased flow into the voided region to continue. Hence, the two-phase region downstream of header 7 is compressed temporarily. An overpressure results, giving a "rebound effect". The upstream fluid then decelerates and the downstream liquid accelerates. Depending on the system conditions, oscillations may damp out and a steady response is obtained, or the oscillations may grow in amplitude until non-linear damping effects become dominant and a limit cycle is reached. Reference 12 provides a method for estimating the oscillation amplitude of the limit cycle in a figure-of-eight loop by examining the void collapse condition.

The nature and existence of oscillations depend on many factors.

The main ones are the loop void fraction, the location of the void, the initial (primary and secondary) test conditions, the net input power (i.e., after accounting for heat losses, if any), and details of the perturbation (such as the location and rate of draining, length of the interval between draining operation) that induces the oscillations.

Test T8805 is an example of a test with quasi-steady header-to-header pressure differentials following intermittent draining (shown in Figure 4). Immediately following a drain, the void fraction was highest in the piping in the vicinity of header 7 (the draining header). After the system was given sufficient time to stabilize, this void was "distributed" evenly between the two core passes, and the thermalhydraulic behaviour of the two core passes until the onset of channel flow reversal was essentially the same. The measured header-to-header pressure drop was relatively steady, and the magnitude of fluctuations, if any, was small when compared with the average values.

Test T8809 is an example of a test with highly oscillatory header-to-header pressure differentials following intermittent draining (shown in Figure 5). It is inferred that the effect of successive removal of the loop liquid inventory from header 7 was to induce larger and larger oscillations in the header-to-header pressure differential in a core pass, while the average header-to-header pressure differential remained close to zero. The header-to-header pressure differential did not stabilize about some steady values but fluctuated in time. Furthermore, the header-to-header pressure differentials in the two core passes were out-of-phase.

The following sections examine the conditions leading to the onset of channel flow reversal under the two types of boundary conditions, i.e., quasi-steady and oscillatory header-to-header pressure differentials. Two topics are of particular interest:

- (a) the magnitude of the negative header-to-header pressure differential required for the onset of channel flow reversal, and
- (b) which of the channels is the first to reverse.

CHANNEL FLOW REVERSAL UNDER QUASI-STEADY HEADER-TO-HEADER PRESSURE DIFFERENTIALS

The four tests (T8805, T8808, T8818 and T8819) in this group have the same nominal primary and secondary conditions. Some relevant results from the experiments are as follows:

- (a) The onset of channel flow reversal occurred at a primary inventory of about 85 to 89 percent.
- (b) The highest elevation channels (5 and 10) were the first to reverse.

It should be noted that for the coolant conditions in these tests, more than 50 percent of the input power (i.e., voltage

times current) is calculated to be lost outside the steam generators (refer to Figure 3 [8]). This magnitude of heat loss is characteristic of the RD-14M facility.

Under steady natural circulation conditions in the loop, the outlet header pressure must exceed the inlet header pressure, otherwise there is insufficient pressure head to drive flow over the steam generators. As the liquid inventory in the loop is continually reduced, the header-to-header pressure differentials become more and more negative, as shown in Figure 4 for test T8805. The basic mechanism appears to be well-understood and is as follows [3,6,7,13]. Draining produced two important effects:

- (a) draining led to a reduction in the liquid inventory. Initially, this led to a decrease in the fluid density in the hot leg side of the loop, thereby increasing the density gradient between the hot and cold leg sides. At the same time, the pressure drop in sections of the loop was increased due to the presence of increased voids. During the first few draining operations, the increased density gradient was able to overcome the increase in two-phase pressure drop, and the loop flow increased.
- (b) draining resulted in the depressurization of the primary heat transport loop close to the pressure of the secondary side in these tests. This led to a gradual reduction of the temperature gradient for heat transfer from the primary to secondary sides.

It is postulated that with further draining, the combination of increased void together with the decreased efficiency of the secondary side to condense the incoming steam caused the length of two-phase region to extend beyond the top of the steam generator U-tubes, and the density gradient between the hot and cold leg sides began to diminish. Further draining from this point onwards further degraded the density gradient for forward flow, while the two-phase pressure drop continued to increase. The header-to-header pressure differential became increasingly negative and the loop flow continued to decrease (see Figure 4). A quantitative model [13] of the above-header components has been set up to simulate the increasingly negative header-to-header pressure differentials as the liquid inventory is reduced. By modelling the above mechanism, agreement between model predictions and experimental results were obtained.

When the header-to-header pressure differentials are relatively steady, the following flow-reversal criterion based on quasi-steady conditions is used: the prevailing header-to-header pressure differential ($P_{IH} - P_{OH}$) must be sufficiently negative to overcome the forward driving force resulting from the density gradient between the inlet and outlet feeders. Mathematically, the requirement can be expressed as:

$$P_{OH}(t) - P_{IH}(t) > \int [\rho_{IF}(z,t) - \rho_{OF}(z,t)] g dz \quad \text{Eq. 1}$$

where $P_{IH}(t)$, $P_{OH}(t)$ are the inlet and outlet header

pressures, respectively, at time t ,
 $\rho_{IF}(z,t)$, $\rho_{OF}(z,t)$ are the fluid densities in the inlet
 and outlet feeders, respectively, at elevation z and
 time t ,
 g is the acceleration due to gravity, and
 the integral on the right hand side is evaluated over
 the vertical distance from the channel to the headers.

The above criterion simply states that for the flow in a channel
 to reverse, the net force on the fluid in the channel must be in
 the reverse direction. As the fluid velocities in the feeders
 and channels around the onset of channel flow reversal were
 observed to be relatively small, frictional effects have been
 neglected in the above criterion. This criterion is consistent
 with earlier analyses [6,14].

Using the quasi-steady flow-reversal criterion, we define a
 header-to-header pressure differential required for channel flow
 reversal, ΔP_{rev} , as follows:

$$\Delta P_{rev}(t) = - \int [\rho_{IF}(z,t) - \rho_{OF}(z,t)] g dz \quad \text{Eq. 2}$$

With this definition, the quasi-steady flow-reversal criterion
 can be restated as follows: When $\Delta P_{HH} > \Delta P_{rev}$, forward flow is
 predicted. When $\Delta P_{HH} < \Delta P_{rev}$, reverse flow is predicted. Under
 two-phase natural circulation conditions (assuming homogeneous
 two-phase flow) and before the onset of channel flow reversal in
 these tests, the following approximations can be made:

$$\rho_{IF} \approx \rho_f$$

$$\rho_{OF} = \langle \alpha_{OF} \rangle \rho_g + (1 - \langle \alpha_{OF} \rangle) \rho_f$$

Thus, ΔP_{rev} can be approximated as

$$\Delta P_{rev}(t) \approx - \langle \alpha_{OF}(t) \rangle (\rho_f - \rho_g) g h \quad \text{Eq. 3}$$

where $\langle \alpha_{OF}(t) \rangle$ is the average void fraction of the fluid in the
 outlet feeder at time t , and h is the elevation difference
 between the channel and the headers. In general, $\langle \alpha_{OF}(t) \rangle$ is a
 function of the outlet feeder geometry (including elevation and
 cross-sectional area changes), the channel power, previous
 operating history of the channel, i.e., $\Delta P_{HH}(t)$ at earlier times,
 and system conditions, e.g. ρ_f , ρ_g and h_{fg} .

The instantaneous void fraction of the fluid in the channel exit
 was estimated from linear interpolation of the gamma densitometer
 readings between the empty and full pipe readings. To obtain the
 average void fraction of the fluid in the outlet feeder, the
 fluid void fraction at the channel exit is averaged in the
 appropriate manner accounting for elevation and cross-sectional
 area changes in the outlet feeder. Table 2 shows the lengths of
 the outlet feeders for the ten channels and the estimated

averaging periods required assuming a typical volumetric flow rate of 0.1 L/s. When the void fraction is a relatively steady function of time, the average outlet feeder void fraction is not sensitive to the length of the averaging periods used, and thus the details of the outlet feeder geometry.

Figure 6 shows a comparison of the header-to-header pressure differential required for flow reversal to occur, ΔP_{rev} , and the experimentally measured pressure differential between headers 6 and 7, ΔP_{HH} , for channel 5 in test T8805.

From Figure 6, it is observed that at the beginning of the test there is a brief period during which $\Delta P_{HH} < \Delta P_{rev}$. This anomalous result is attributed to the fact that during this period, the loop is in single-phase thermosiphoning and use of Eq. 3 is invalid.

During the period from the start of the first drain to the end of the sixth drain (primary inventory from 100 to 88 percent), it is observed that $\Delta P_{HH} > \Delta P_{rev}$. For the time period from the end of the sixth drain to the beginning of the seventh drains, ΔP_{HH} becomes comparable to ΔP_{rev} , or $\Delta P_{HH} < \Delta P_{rev}$. Experimentally, onset of channel flow reversal was observed to occur during the seventh drain (primary inventory of 83 percent). Considering the instrument uncertainties and the approximations used to obtain the results, the agreement between the experimental data and the quasi-steady flow-reversal criterion is quite good. Applying the quasi-steady flow-reversal criterion to the 4 quasi-steady tests in this group, and using the actual header-to-header pressure differentials, the inventory fractions at the onset of channel flow reversal determined with the above criterion are estimated to be within 3 percentage points of the experimentally measured inventory fractions (see Table 3). Alternatively, the values of ΔP_{rev} at the onset of channel flow reversal determined using the above criterion are within 18 percent of those of the experimentally measured ΔP_{HH} for the 4 quasi-steady tests.

As noted earlier, the header-to-header pressure differential required for channel flow is dependent on the past operating history of the channel. For example, the magnitude of the ΔP_{rev} for a particular channel depends on the rate at which a change in the header-to-header pressure differential is brought about. If the change in header-to-header pressure differential is brought about at a very slow rate, allowing sufficient time for the fluid density in the outlet feeders to adjust to the new flow rates through the channel, then the channel flow would slow down very gradually, and the quality of the fluid leaving the channel would increase slowly as a result. Ultimately, the outlet feeder would be almost completely voided, while the channel flow would drop to a very small value. In this case, the header-to-header pressure differential required to reverse the flow direction would be approximately $(\rho_f - \rho_g)gh$. In these relatively steady experiments, it is found that the header-to-header pressure

differentials at the onset of channel flow reversal are smaller than the above value because the fluid void fraction in the outlet feeder is typically much less than unity. Figure 7 shows the outlet feeder average void fraction in channel 5 for test T8805. It is observed that just prior to the onset of channel flow reversal, the average void fraction in the outlet feeder was between 30 to 60 percent. It is concluded that the rate of change of the header-to-header pressure differentials with time in these experiments is rapid compared to the transit times through the channels and the outlet feeders. Consequently, the fluid densities in the outlet feeders appears to be "frozen" at their old values just prior to the onset of channel flow reversal.

It is noted that the onset of channel flow reversal in many tests (3 out of 4) occurred during a draining operation. This is not surprising since it is during a draining operation that the header-to-header pressure differentials were changing rapidly in time.

According to the above criterion, the highest elevation and lowest power channels should be the first to reverse (refer to Eq. 3). In these RD-14M tests, the flow resistances and the input powers to the ten channels were scaled in such a way that the qualities of the fluid leaving the channels were roughly the same. Figure 8 shows the outlet feeder average void fraction for channels 5 to 9 in test T8805 as a function of time. The elevation term (see Table 4) in Eq. 3 is expected to dominate, and the top channels are predicted to be the first to reverse as shown in Figure 9 for test T8805. This is in agreement with the experimental results for the relatively steady tests.

CHANNEL FLOW REVERSAL UNDER OSCILLATORY HEADER-TO-HEADER PRESSURE DIFFERENTIALS

When the header-to-header pressure differentials were oscillatory, the main experimental observations are as follows:

- (a) Onset of channel flow reversal for the 1 MPa tests (T8809 and T8810) occurred at a relatively high primary inventory of 92.6 percent, while onset of channel flow reversal for the 0.1 MPa test (T8804) occurred at a primary inventory of 83.2 percent.
- (b) Even though T8810 was a repeat test of T8809, the first channels to reverse were different for tests T8809 and T8810. Previous analysis did not reveal any consistent pattern regarding which of the channels would be the first to reverse for these tests.

It is estimated that heat losses from components other than the steam generators account for more than 35 percent of the input power (i.e., voltage times current) in T8809 and T8810, and more than 18 percent of the input power in T8804 (refer to Figure 3 [8]).

Figure 5 shows that in test T8809 large out-of-phase oscillations in the header-to-header pressure differentials were produced during and after each draining, while Figure 10 shows that in test T8804 smaller header-to-header differential pressure oscillations were produced. Not surprisingly, onset of channel flow reversal occurred at a higher inventory in test T8809 than in test T8804.

When the header-to-header pressure differentials are oscillatory, the quasi-steady flow-reversal criterion is no longer sufficient for predicting the onset of channel flow reversal. A dynamic stability analysis that models the transient and feedback processes occurring inside the feeders and channels is required. The development of a dynamic flow-reversal criterion is in progress. As a temporary measure, we have applied the quasi-steady flow-reversal criterion to tests with oscillating header-to-header pressure differentials. Some insights can be gained from these tests by using this simple criterion. The inadequacy of the quasi-steady flow-reversal criterion for tests with oscillating header-to-header pressure differentials is also demonstrated.

Figure 11 shows a comparison of the header-to-header pressure differential, ΔP_{rev} , required for channel flow reversal from Eq. 3 for channel 8 in test T8809 and the experimentally measured pressure differential, ΔP_{HH} , between headers 6 and 7. Using the methodology developed in the previous section, the outlet feeder void fraction was estimated by averaging the instantaneous fluid void fraction leaving the channel for the time durations shown in Table 2. It is observed in Figure 11 that there are many instances when the values of ΔP_{HH} approach those of ΔP_{rev} . These observations are confirmed by the corresponding slowdowns in the inlet turbine flow meter readings shown in Figure 12. Around 3000 seconds, $\Delta P_{HH} < \Delta P_{rev}$. Flow reversal in channel 8 was observed to occur shortly afterwards.

The net pressure head on the fluid in a given channel is the sum of the header-to-header pressure differential and the density gradient between the inlet and outlet feeders for that particular channel, as shown in Equation 4 below.

$$\Delta P_{net}(t) = \Delta P_{HH}(t) + \int [\rho_{IF}(z,t) - \rho_{OF}(z,t)] g dz \quad \text{Eq. 4}$$

For forward flow, $\Delta P_{net}(t) > 0$. For reverse flow, $\Delta P_{net}(t) < 0$. In these tests, the first term in Equation 4, i.e., the header-to-header pressure differentials, exhibited large amplitude oscillations about zero, while the second term in Equation 4, the density gradient term, also exhibited large amplitude oscillations. Depending on the timing and magnitude of the oscillations for the different channels, the flow in a particular channel may or may not reverse. However, it is clear that under highly oscillatory header conditions, the top channels are not necessarily the first ones to reverse. Some elements of the

above explanation were discussed in references 4 and 7.

In particular, in test T8809, the timing and magnitude of the oscillations in the header-to-header pressure differentials and the density gradient between the inlet and outlet feeders were such that channel 8, not channel 5, was the first to reverse. Figure 13 shows the inlet turbine flow meter readings for channels 5 and 8 in test T8809. It is observed that the magnitude of the channel flow oscillations in channel 8 was much larger than that in channel 5. (It should be noted that channel 8 has the smallest combined flow resistance amongst channels in the same core pass, as shown in Table 5). Corresponding to these large channel flow oscillations, single-phase liquid was detected at the outlet of channel 8 much more frequently than from channel 5, as shown in Figures 14 and 15. Consequently, the average outlet feeder void fraction, $\langle \alpha_{of} \rangle$, for channel 8 was often smaller than that for channel 5 (see Figure 16). Consequently, the header-to-header pressure differential required for channel flow reversal, ΔP_{rev} , for channel 8 was often smaller than that required for channel 5 for certain time intervals.

Figure 17 shows the estimated header-to-header pressure differential, ΔP_{rev} , required for channel flow reversal for channels 5 to 9 based on Eq. 3 in test T8809. It is observed that using the present quasi-steady channel flow reversal criterion, it is not possible to determine which of the channels would be the first to reverse. This is to be expected. Development of a dynamic model accounting for transient and feedback effects is in progress.

MODELLING AND RESULTS

In the previous sections, the condition for the onset of channel flow reversal is expressed in terms of the header-to-header pressure differential. In practice, the header-to-header pressure differential in any RD-14M test is not known a priori. To bridge this gap, a model of the thermalhydraulic behaviour of the below-header components in the RD-14M loop has been developed. The intention is to couple this "below-header" model with the "above-header" model developed by Fung [13] to predict the primary inventory at the onset of channel flow reversal for these tests. This work is in progress. In this section, the current status of this task is presented.

Information on the flow resistances and dimensions of the loop was obtained from references 1 and 15. For simplicity, homogeneous two-phase flow was assumed. It is further assumed that changes to the header-to-header pressure differential are brought about instantaneously (i.e., step-function increase or decrease in the externally imposed header-to-header pressure differential).

Figure 18 shows the predicted fluctuation in header-to-header pressure differential required for channel flow reversal in test section 5 as a function of the average header-to-header pressure differential at a net channel power (i.e. input channel power minus estimated heat losses) of 10, 20, and 30 kW, respectively and a pressure of 5 MPa. In these tests, fluctuations or oscillations in ΔP_{HH} can arise from several sources, such as: (a) from the draining operation, (b) from the system conditions following a drain, and (c) from changes occurring in the secondary side (e.g. intermittent operation of the jet condenser).

In those tests with relatively steady header-to-header pressure differentials, the ΔP_{HH} was observed to become more negative as the liquid inventory was reduced. Figure 18 shows that as the average header-to-header pressure differential, ΔP_{HH} , becomes more negative, the fluctuation in ΔP_{HH} required for channel flow reversal is predicted to be smaller. Eventually, a small fluctuation, say ± 2 kPa, would be sufficient to trigger a channel flow reversal. This result is consistent with the experimental observations.

In those tests with oscillatory header-to-header pressure differentials, e.g. test T8809, ΔP_{HH} was observed to oscillate about zero. Figure 18 shows that when the average header-to-header pressure differential is around zero, much larger fluctuations, on the order of ± 15 kPa, are predicted to be required to trigger the onset of channel flow reversal. This result is consistent with the experimental observations as well.

The present model can also be used to assess quantitatively the effect of heat losses on the channel flow reversal behaviour. Figure 19 shows the predicted fluctuation in header-to-header pressure differential required for reversing the direction of flow in channel 5 as a function of the net channel power at an average header-to-header pressure of -10 kPa and a pressure of 5 MPa. It is observed that as the net channel power is decreased, the magnitude of the fluctuation in ΔP_{HH} required for channel flow reversal is also reduced.

In the future, it is planned to integrate the present "below header" model with an "above-header" model of the RD-14M loop to predict the primary inventory at the onset of channel flow reversal. Once an integrated model is in place, the effect of heat losses on the primary inventory at the onset of channel flow reversal can be predicted.

SUMMARY

The status of a detailed analysis of the T88 series of partial inventory thermosiphoning RD-14M tests has been presented. The approach used is to develop a relatively simple model that

"captures" as many of the important phenomena as possible. Because of the very high heat losses in these RD-14M tests, the present work concentrated on the high power (160 kW/pass) tests. In particular, the conditions leading to the onset of channel flow reversal are examined.

These tests are grouped together according to whether the behaviour of the header-to-header pressure differentials were either relatively steady or oscillatory.

A conceptually simple flow-reversal criterion based on quasi-steady conditions is used in these tests: the prevailing header-to-header pressure differential must be sufficiently negative to overcome the forward driving force resulting from the density gradient between the inlet and outlet feeders.

In those tests with relatively steady header-to-header pressure differentials, the header-to-header pressure differentials were observed to become increasingly negative as the loop liquid inventory was reduced. The mechanisms responsible for the increasingly negative header-to-header pressure differential were described. Using the quasi-steady flow-reversal criterion, the header-to-header pressure differential required for the onset of channel flow reversal, ΔP_{rev} , was computed as a function of time. Onset of channel flow reversal occurs when $\Delta P_{HH} < \Delta P_{rev}$. Applying the above criterion to these tests, the top channels are expected to be the first to reverse. This result is in agreement with the experimental results.

For those tests with oscillatory header-to-header pressure differentials, the amplitude of these oscillations was observed to increase as the loop liquid inventory was reduced. A qualitative explanation for the oscillatory behaviour of the loop was given. Using the quasi-steady flow-reversal criterion, the header-to-header pressure differential required for the onset of channel flow reversal, ΔP_{rev} , was again computed as a function of time. When the experimentally measured header-to-header pressure differential approached ΔP_{rev} , temporary flow slowdowns were observed. When $\Delta P_{HH} < \Delta P_{rev}$, the onset of sustained channel flow reversal was observed. By applying the quasi-steady flow-reversal criterion to these tests, it is shown the top channels are not necessarily the first to reverse. However, the present methodology is unable to predict which of the channels is the first to reverse in these tests. A dynamic flow-reversal criterion, accounting for transient and feedback processes, is being developed.

A model of the below-header components in the RD-14M loop is under development. The model has been used to predict the fluctuation in header-to-header pressure differential, ΔP_{HH} , required for channel flow reversal as a function of the average ΔP_{HH} . Model predictions are consistent with experimental results. The model also predicts that smaller fluctuations in

ΔP_{HH} are required for channel flow reversal as the net channel power is decreased. It is planned to integrate the present "below-header" model with the "above-header" model by Fung [13] to predict the primary inventory at the onset of channel flow reversal.

REFERENCES

1. MCGEE, G.R., SPITZ, K.O., BORGFORD, T.A., FINDLAY, J.W., HOOD, B.E., and THOMSON, R.G., "RD-14M Facility Description," AECL report COG-88-42, July 1989.
2. INGHAM, P.J., "Natural Circulation Experiments in the RD-14 Multiple Channel Thermalhydraulics Loop," presented at the 15th Simulation Symposium on Reactor Dynamics and Control, Mississauga 1989 May 1-2.
3. MALLORY, J.P. and INGHAM, P.J., "CATHENA Simulation of Thermosiphoning in a Multiple-Channel Pressurized Water Test Facility", presented at 10th Annual Conference of the CNS, Ottawa, 1989 June 4-7.
4. GULSHANI, P., BARKMAN, J.N., HUYNH, H., WRIGHT, M.A., "Status of Natural Circulation Experiments in Multiple Channel RD-14M Test Facility", paper presented at 3rd CNS/ANS International Conference on Simulation Methods in Nuclear Engineering, Montreal, Quebec, 1990 April 18-20.
5. HO, S.F., "Summary of Selected Natural Circulation Tests", personal communication to W.I. Midvidy, June 29, 1990.
6. P.J. INGHAM, A.J. MELNYK, AND T.V. MURRAY, "Natural Circulation Experiments in RD-14M With Emergency Coolant Injection," Proceedings of International Topical Meeting on Safety of Thermal Reactors, p. 504-516, Portland, Oregon, U.S.A., July 21-25, 1991.
7. PASCOE, J., "Onset of Bidirectional Flow in RD-14M Partial Inventory Thermosiphoning Experiments T8801-T8820," personal communication to J.C. Luxat, March 1, 1991.
8. HO, S.F., "Heat Loss Characteristics of the RD-14M Loop," personal communication to W.I. Midvidy, February 14, 1990.
9. GULSHANI, P., "A Figure-of-Eight Stability Model - Thermosiphoning and Normal Operation Modes," TDAI-306, 1983.
10. ARDRON, K.H., and KRISHNAN, V.S., "Stability of a Two-Phase Natural Circulation Loop with Figure-of-Eight Symmetry," AECL-7958, 1983.
11. GARLAND, W.J., and PANG, S., "CANDU-600 Heat Transport

- System Flow Stability," *Nuclear Technology*, Vol. 75, 1986.
12. TRAN, F.B.P., BOWMAN, W.C., MUZUMDAR, A.P., ARCHINOFF, G.H., "Methodology for Assessing Figure of Eight Type Flow Oscillations in CANDU Primary Heat Transport Systems," Proceedings of the 10th Annual CNA/CNS Conference, 1989.
 13. FUNG, K.K., "An Analysis of RD14M Natural Circulation Tests," personal communication to W.I. Midvidy, 1991.
 14. ONTARIO HYDRO, *Darlington NGS Safety Report*, Appendix D, Volume 3, Chapter 3, 1990.
 15. MCGEE, G.R., "Hydraulic Resistances of RD-14M Primary Loop Components," AECL draft report COG-91-155, 1991.

TABLE 1
 Brief Summary of Test Results at 160 kW/Pass & Surge Tank Isolated
 from Heat Transport Loop

Test #	Pressure (MPa)		Onset of Flow Reversal		Power Trip	
	Primary	Secondary	Inventory, %	Channel No.	Inventory, %	Chann el No.
T8805	7.0	4.5	86.1 during last drain	10,5	83.0	9
T8808	7.0	4.5	85.3 during last drain	10,5	81.5	9
T8818	7.0	4.5	89.3 during last drain	10,5	87.4 due to high boiler FW inlet temperature	-
T8819	7.0	4.5	88.0 after 7th drain	10,5	79.6	11
T8809 ¹	5.0	1.0	92.6 after 4th drain	12,8	90.7	8
T8810	5.0	1.0	92.6 after 4th drain	5,14	87.0	11
T8804	5.0	0.1	83.2 during 7th drain	6,8,11, 12	65.8	8

Notes:

¹ repeat of T8805 with slower drain rates

TABLE 2
Lengths and Estimated Averaging Periods for RD-14M Channels

Channel No.	Length of Outlet Feeder (m)	Averaging Period (s)
5,10	9.2	88
6,11	12.2	118
7,12	19.1	231
8,13	17.1	213
9,14	20.3	196

TABLE 3
Comparison of Experimentally Measured Inventory Fractions at Onset of Channel Flow Reversal with Those Determined Using the Quasi-Steady Flow-Reversal Criterion

Test No.	Experimental Value	Quasi-Steady Flow-Reversal Criterion Value	Difference
T8805	87.6 %	86.1 %	1.5 %
T8808	86.1 %	85.3 %	0.8 %
T8818	90.7 %	89.3 %	1.4 %
T8818	90.7 %	88.0 %	2.7 %

TABLE 4
Elevation Difference Between the Headers and the Channels

Channel No.	Elevation Difference (m)
5,10	4.20
6,11	6.75
7,12	7.05
8,13	7.60
9,14	10.23

Table 5
RD-14M Frictional Resistance Coefficients for Below Header Components [15]

Test Section No.	k_{IF}	k_{ch}	k_{OF}	$k_{total} = k_{IF} + k_{ch} + k_{OF}$
5	3.19	4.12	0.34	7.65
6	3.57	4.50	0.49	8.56
7	0.76	4.45	0.48	5.69
8	0.85	4.05	0.35	5.25
9	3.34	4.14	0.65	8.13
10	3.31	3.82	0.33	7.46
11	2.93	3.79	0.40	7.12
12	0.69	3.63	0.44	4.76
13	0.86	4.13	0.35	5.34
14	3.28	4.30	0.70	8.28

Note: In Reference 15, the frictional resistance coefficient, k , of a component is defined as follows -

$$\Delta P_{fric} = k Q^2$$

where ΔP_{fric} is the frictional pressure drop (in units of m of water)

Q is the volumetric flow rate (in units of L/s)

$$\text{Thus, } \Delta P_{HH} = (k_{IF} + k_{ch} + k_{OF}) Q^2$$

Rearranging,

$$Q = (\Delta P_{HH})^{0.5} / (k_{IF} + k_{ch} + k_{OF})^{0.5}$$

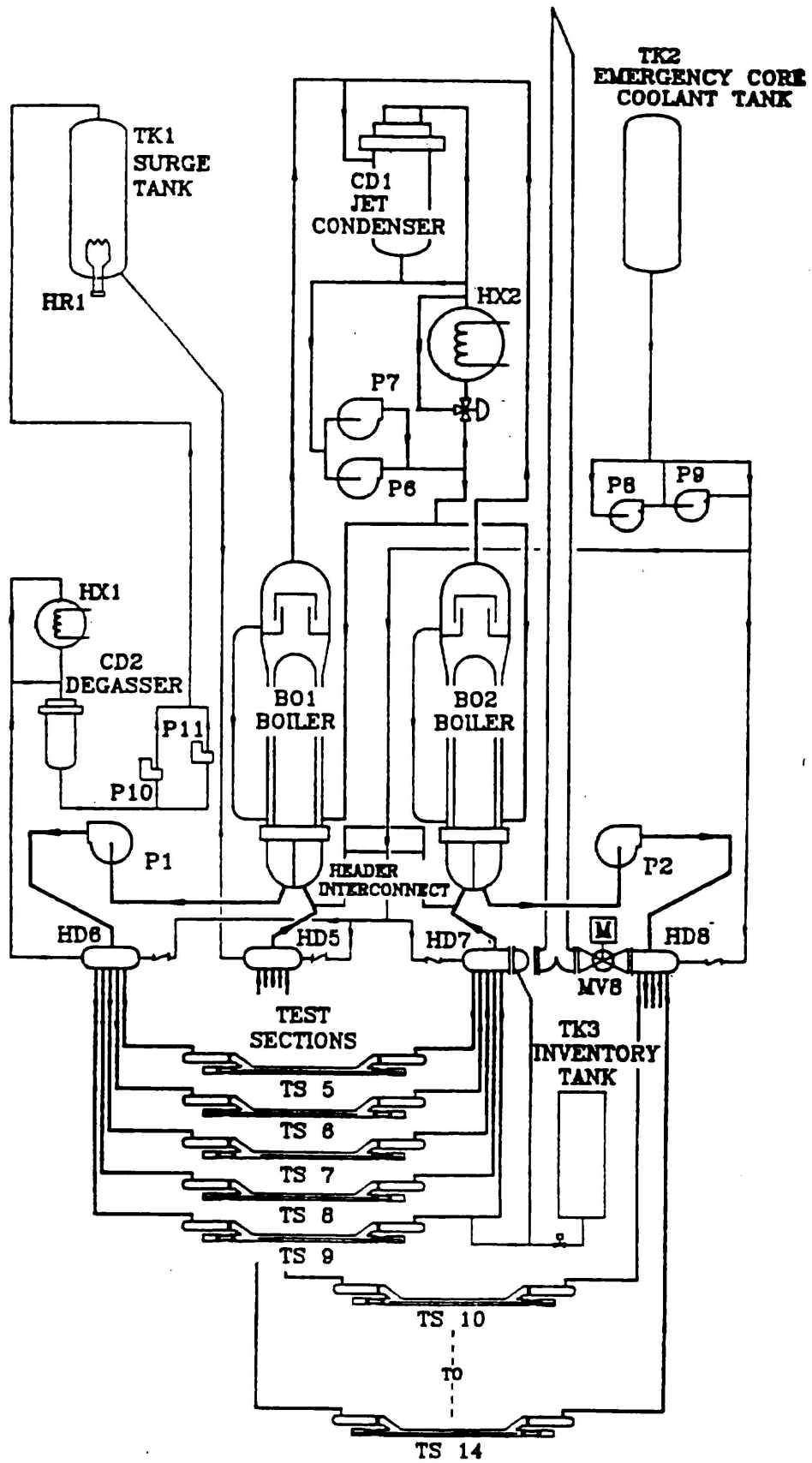


Figure 1. RD-14M Loop Schematic

T8805

9-PT (18-S) AVERAGING

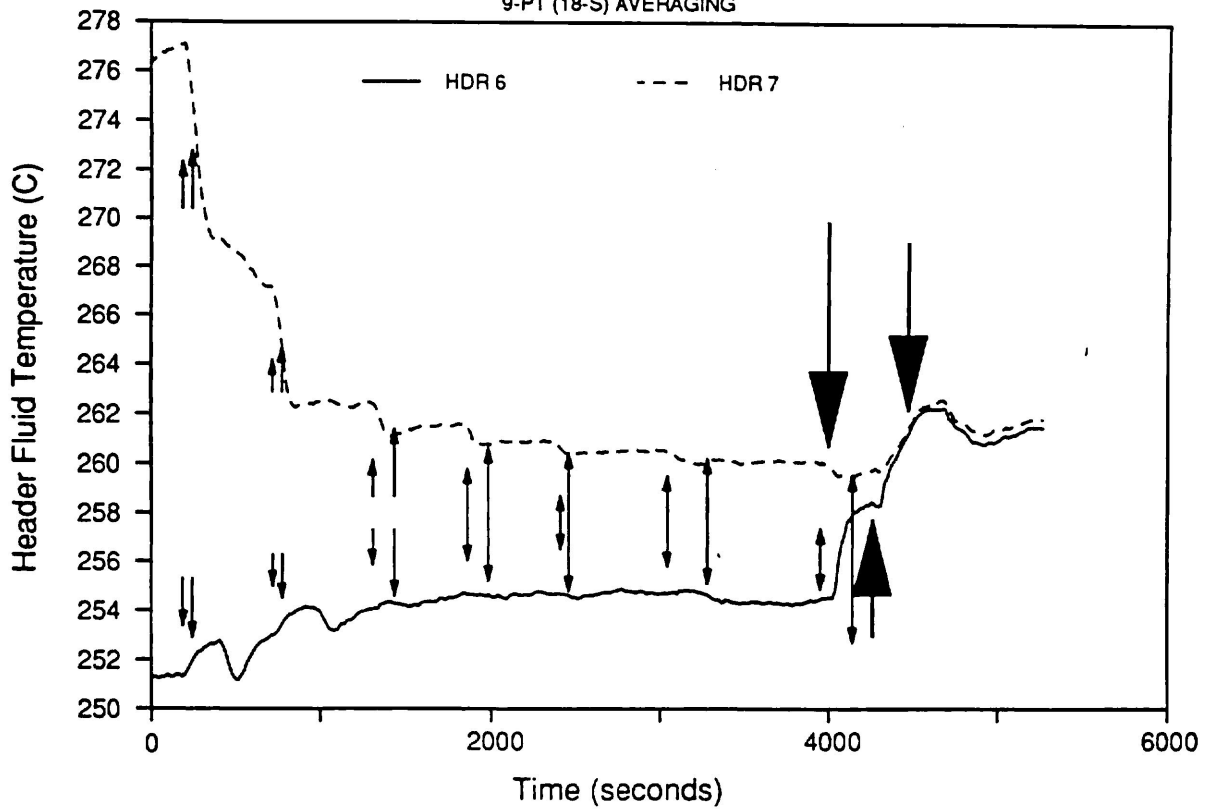
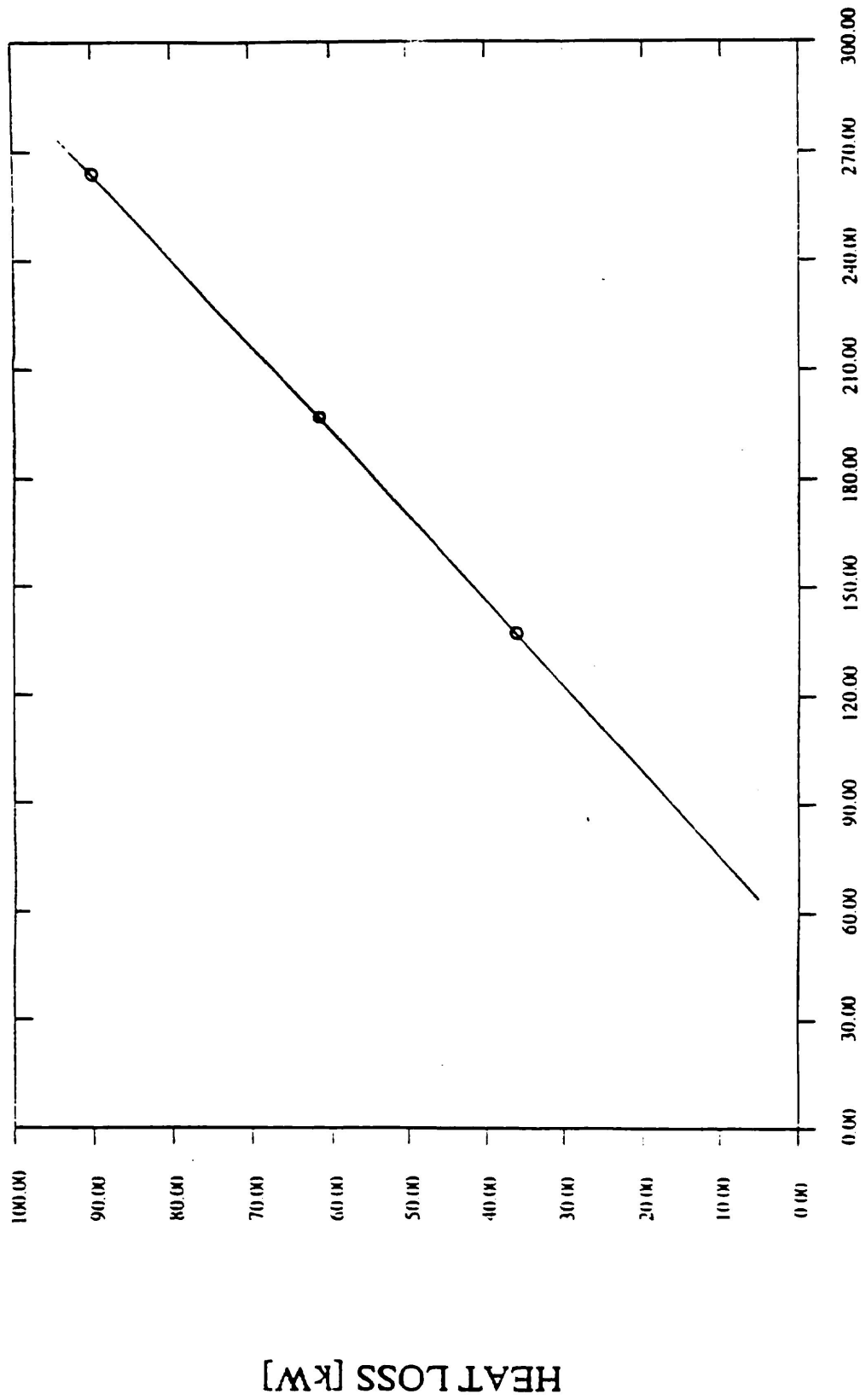


Figure 2. Header Fluid Temperature as a Function of Time in Test T8805.

HEAT LOSS VS LOOP TEMPERATURE



AVE LOOP TEMPERATURE [C]

Figure 3. Estimated Heat Loss Per Pass Versus Average Coolant Temperature in the RD-14M Facility.

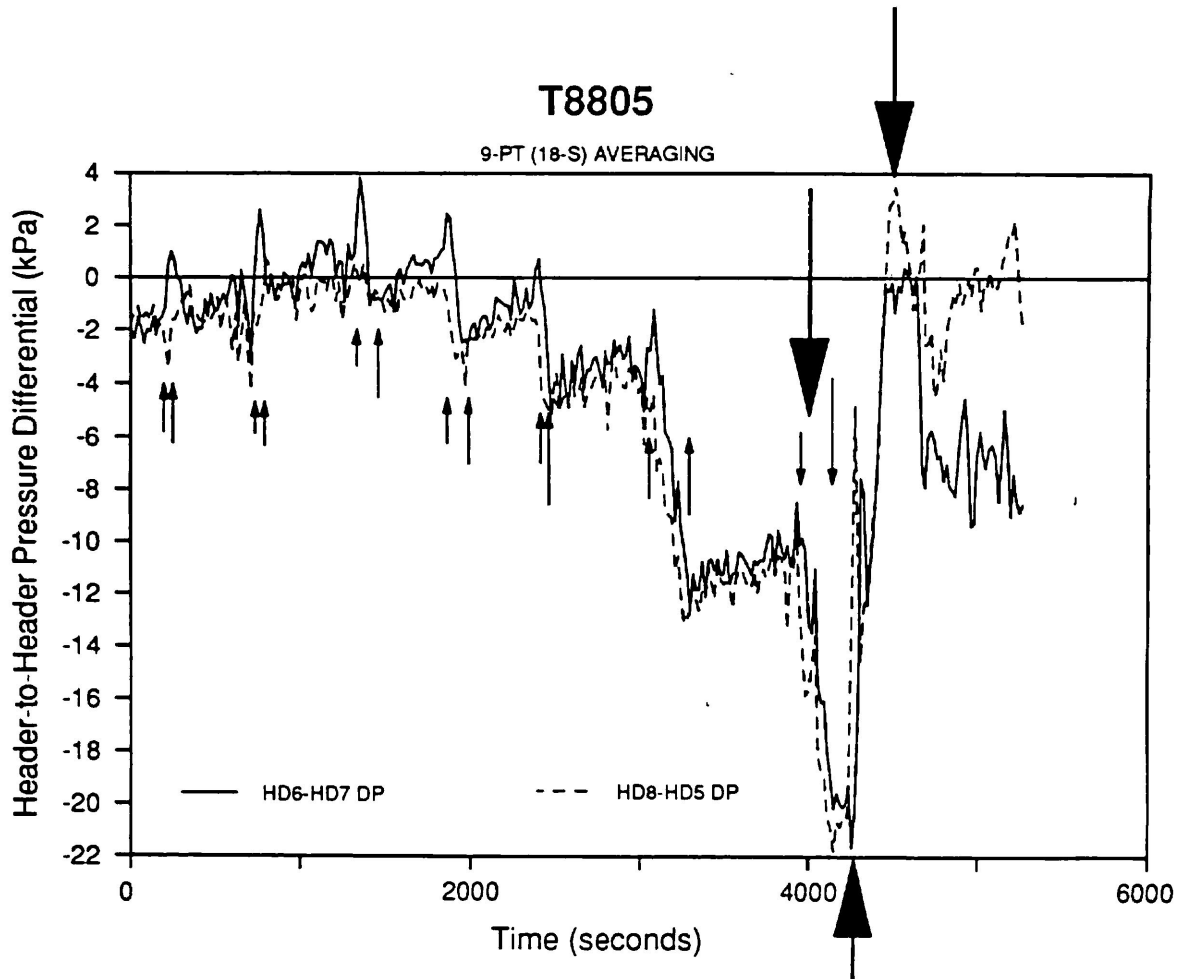


Figure 4. Header-to-Header Pressure Differential as a Function of Time in Test T8805.

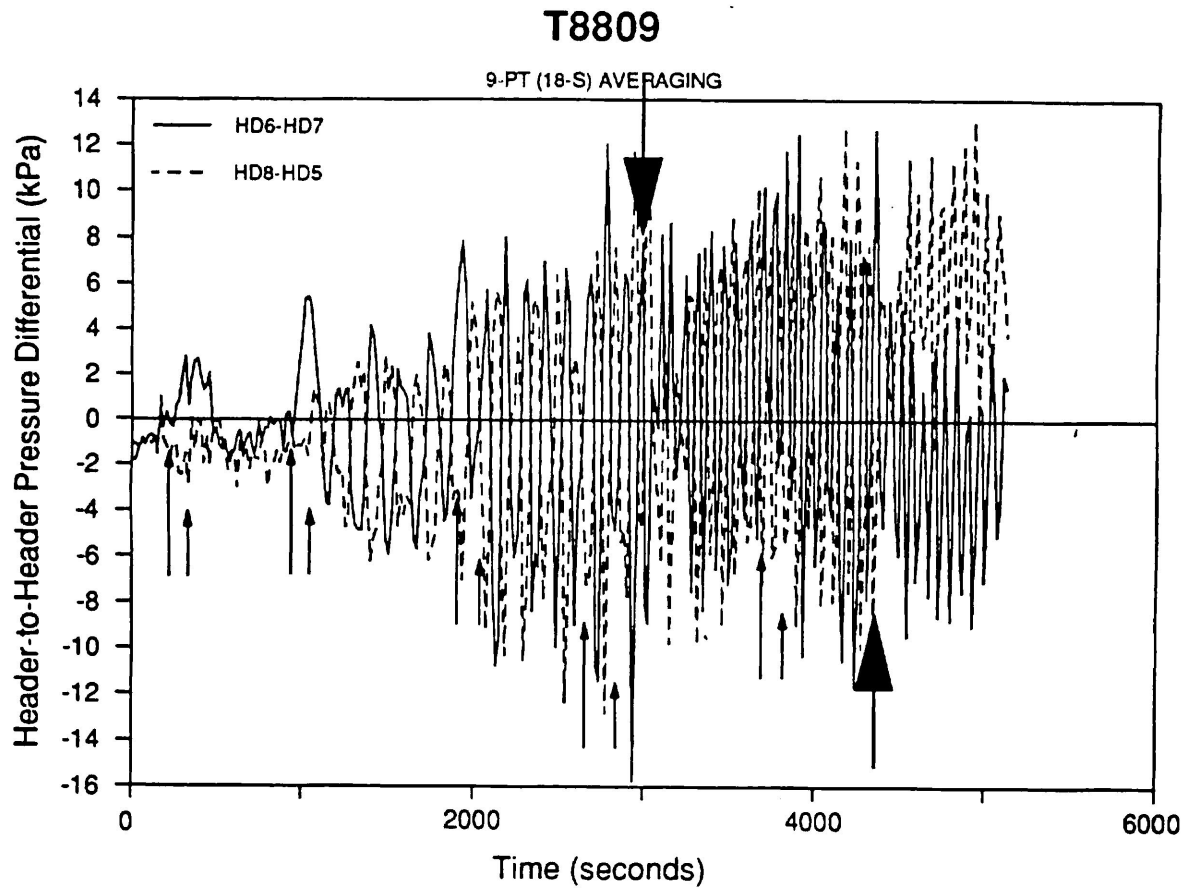


Figure 5. Header-to-Header Pressure Differential as a Function of Time in Test T8809.

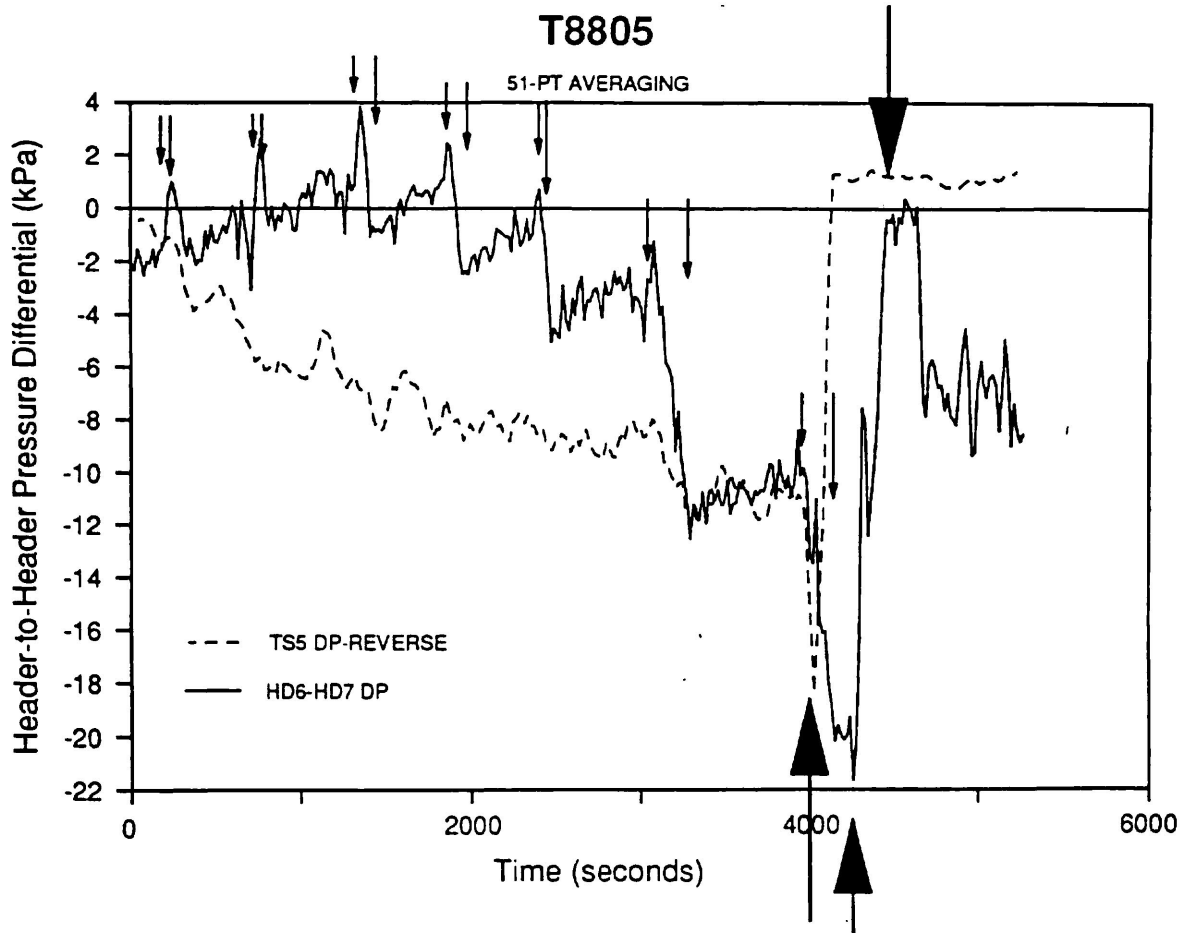


Figure 6. Comparison of Experimentally Measured Header-to-Header Pressure Differential and the Header-to-Header Pressure Differential Required for Channel Flow Reversal for Channel 5 in Test T8805.

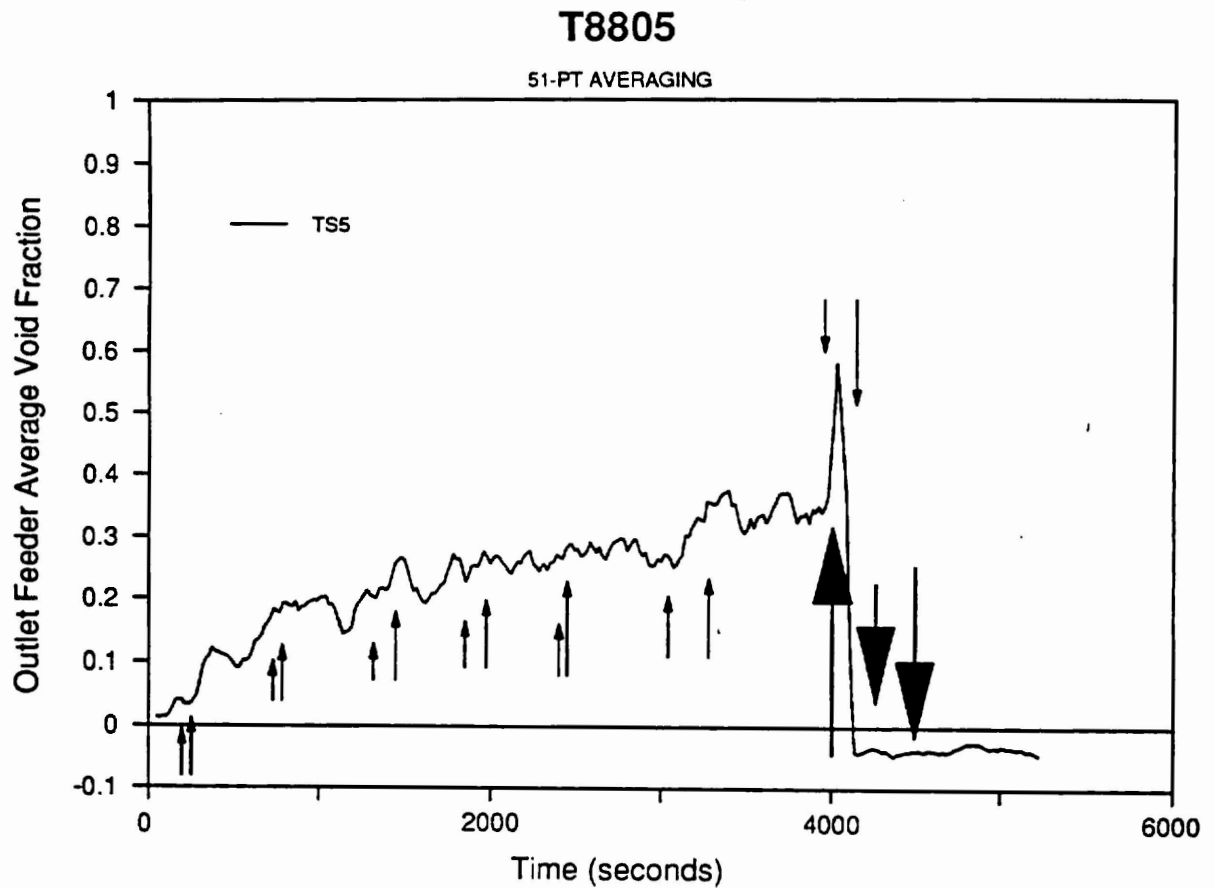


Figure 7. Outlet Feeder Average Void Fraction of Channel 5 as a Function of Time in Test T8805.

T8805

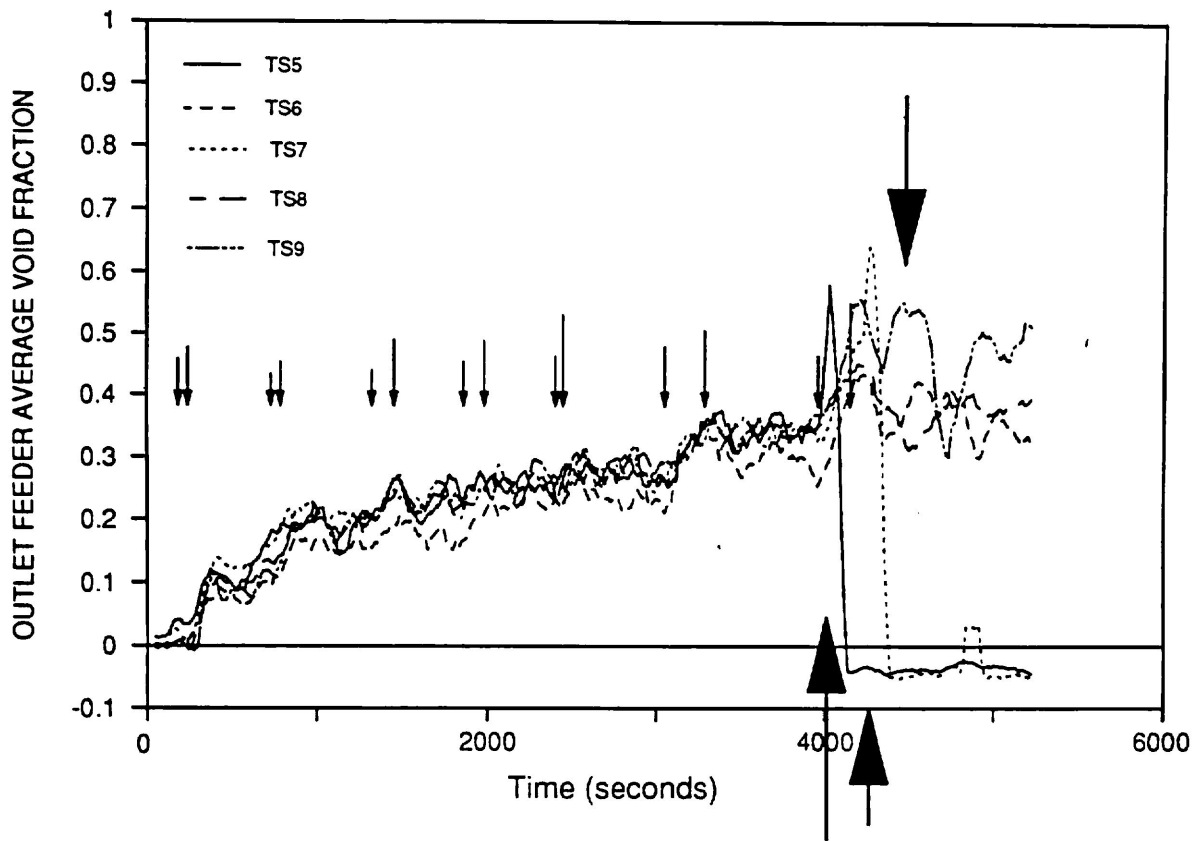


Figure 8. Outlet Feeder Average Void Fraction of Channels 5 to 9 as a Function of Time in Test T8805.

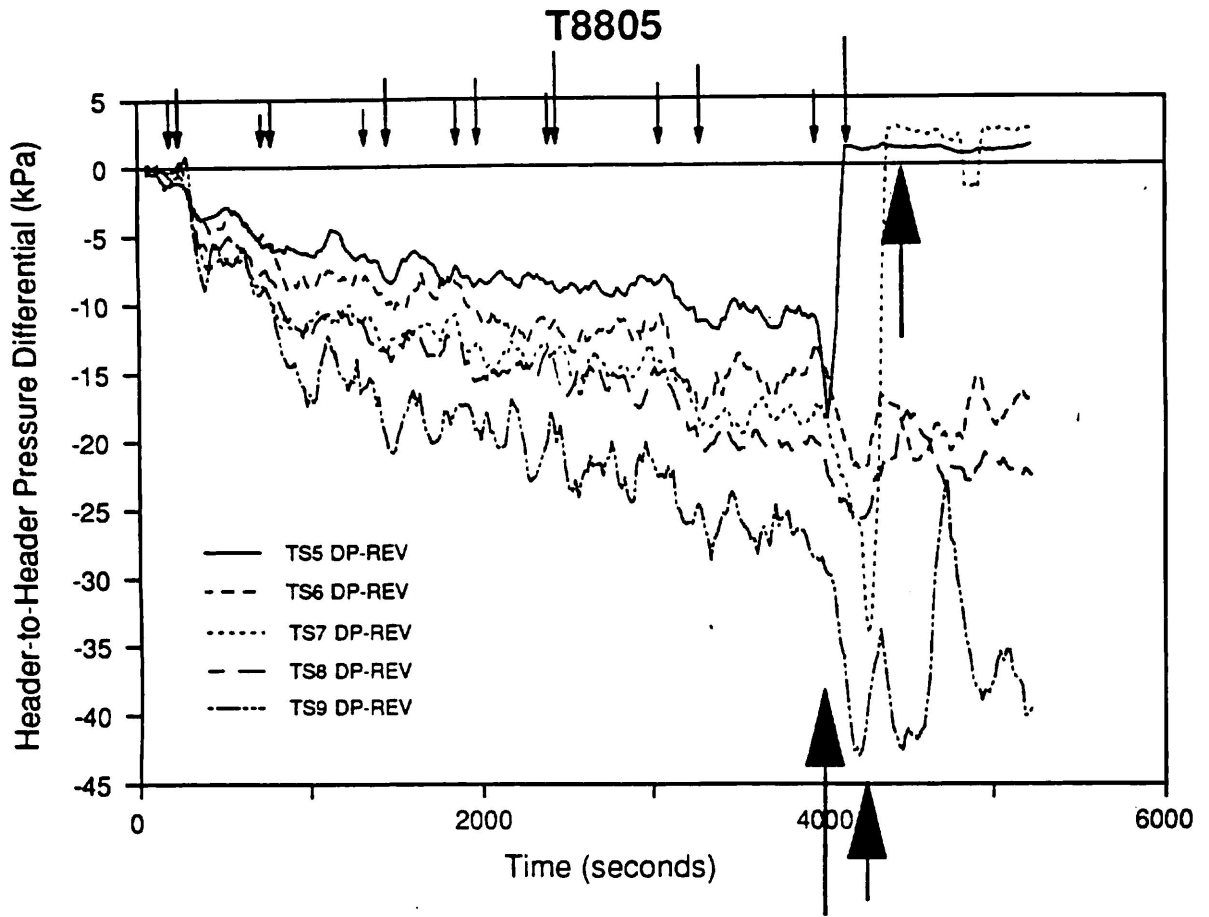


Figure 9. Header-to-Header Pressure Differential Required for Channel Flow Reversal for Channels 5 to 9 as a Function of Time in Test T8805.

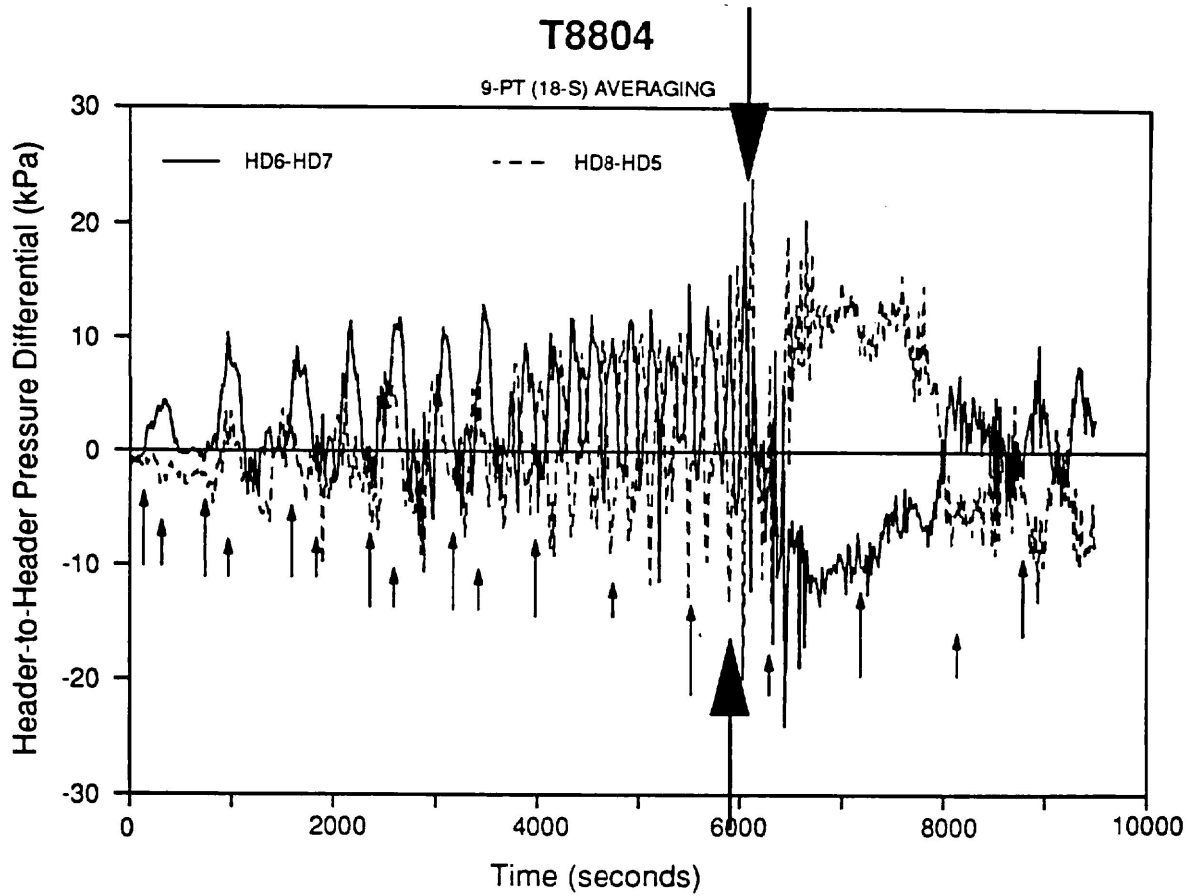


Figure 10. Header-to-Header Pressure Differential as a Function of Time in Test T8804.

T8809

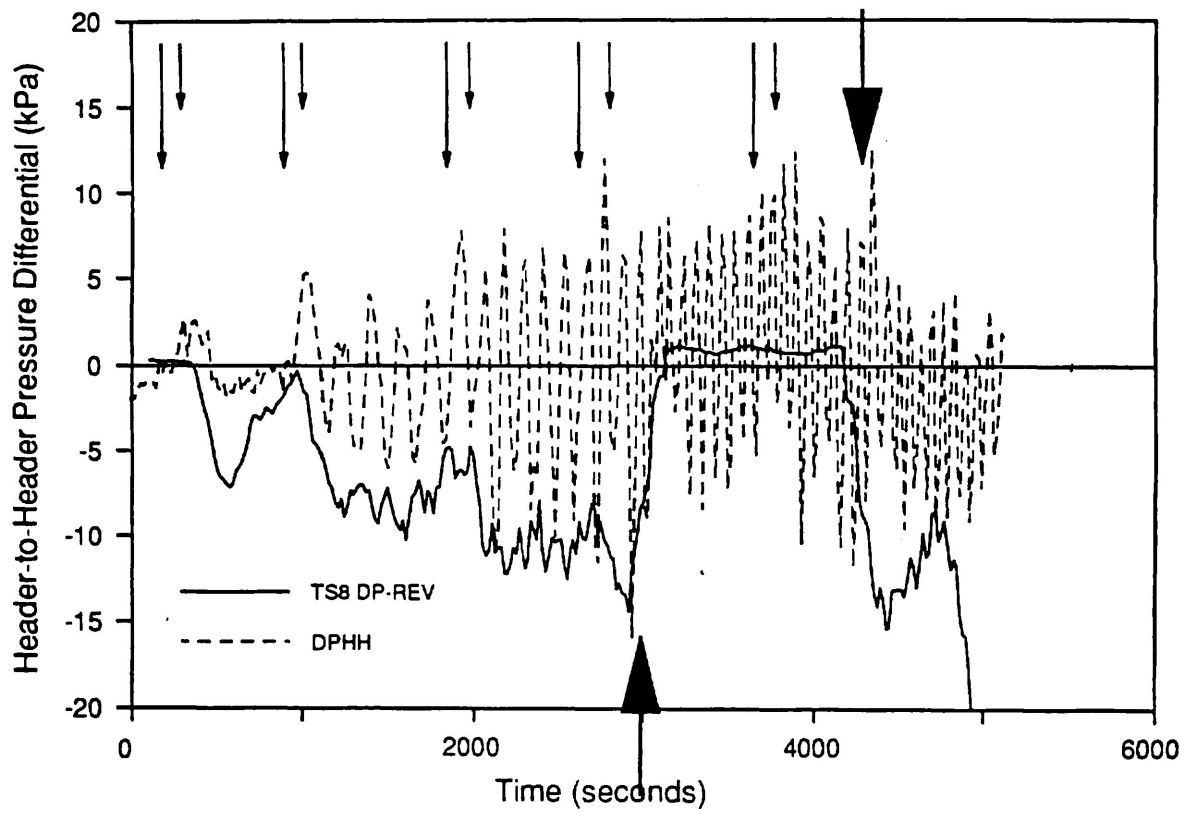


Figure 11. Comparison of Experimentally Measured Header-to-Header Pressure Differential and the Header-to-Header Pressure Differential Required for Channel Flow Reversal for Channel 8 in Test T8809.

T8809

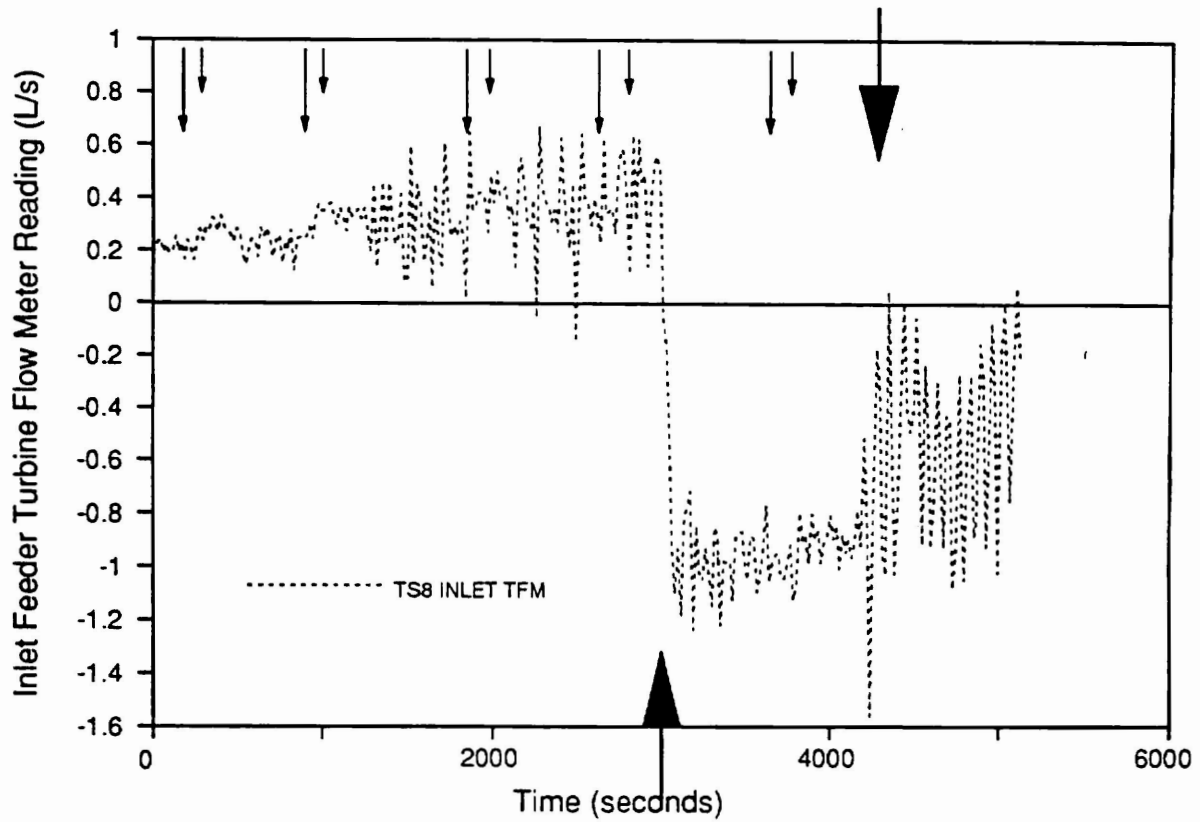


Figure 12. Inlet Feeder Turbine Flow Meter Reading as a Function of Time for Channel 8 in Test T8809.

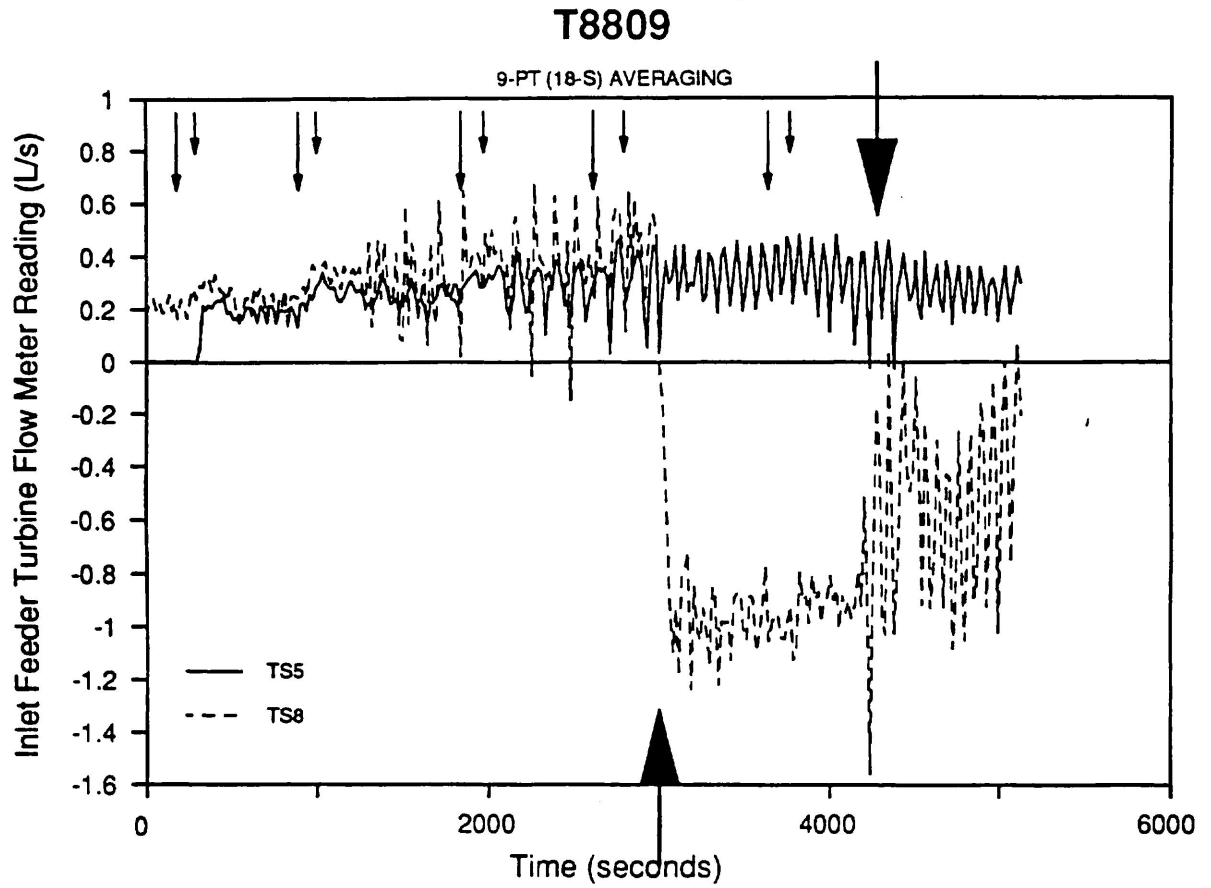


Figure 13. Comparison of Inlet Feeder Turbine Flow Meter Reading for Channels 5 and 8 in Test T8809.

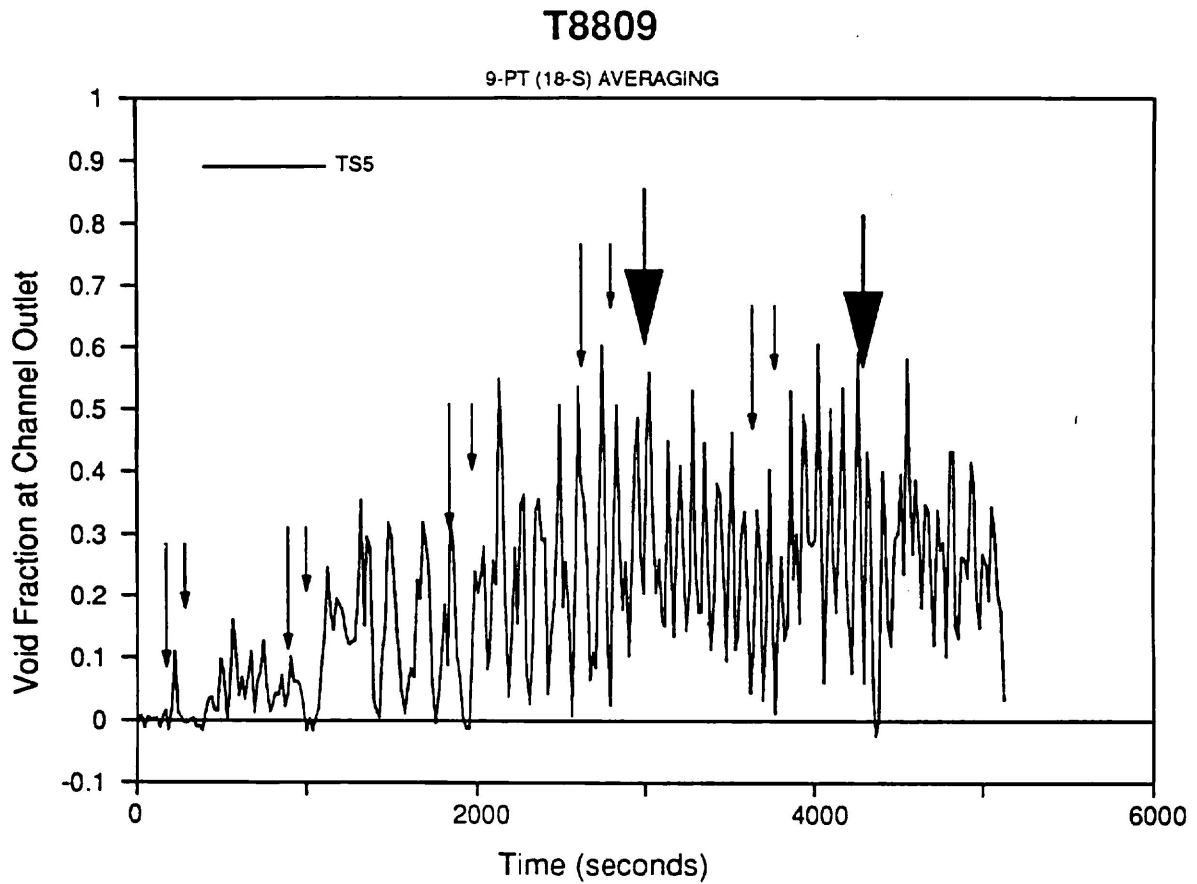


Figure 14. Void Fraction of Fluid Leaving Channel 5 as a Function of Time in Test T8809.

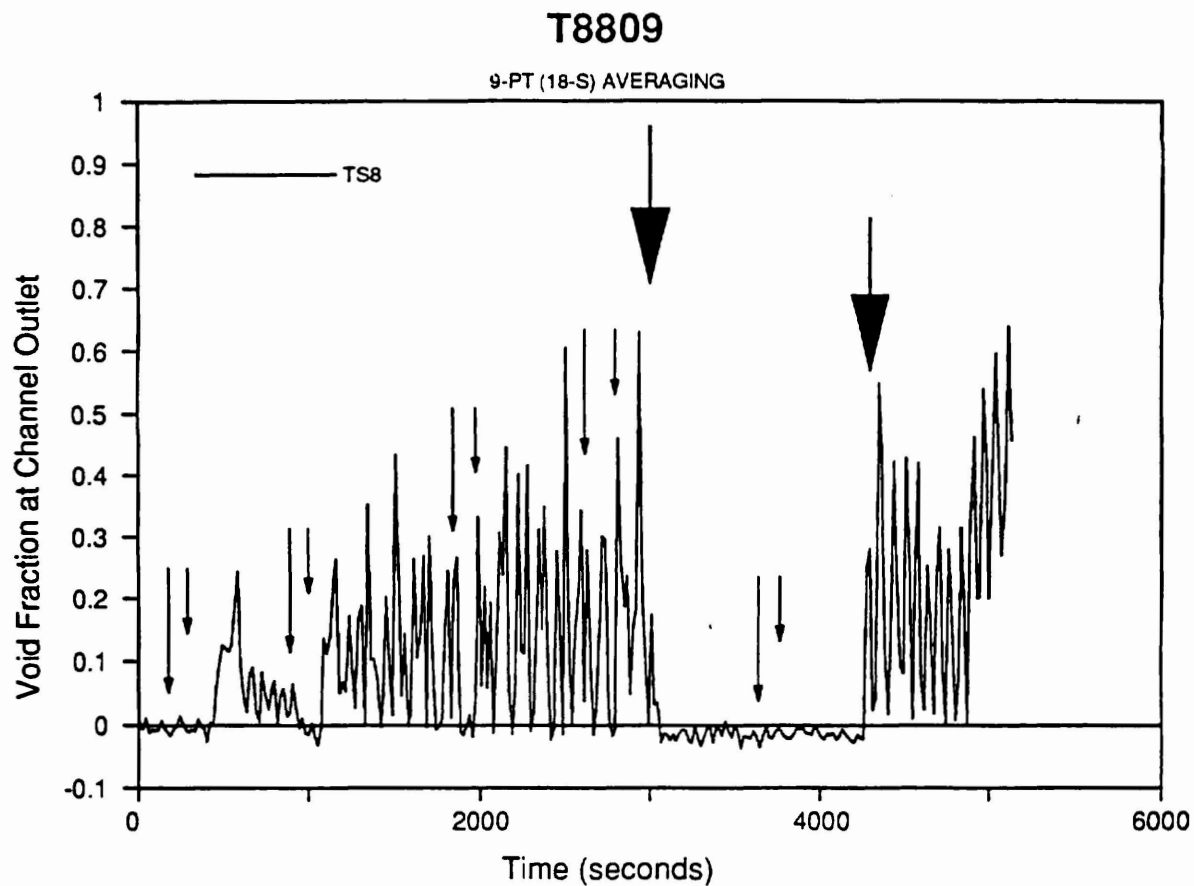


Figure 15. Void Fraction of Fluid Leaving Channel 8 as a Function of Time in Test T8809.

T8809

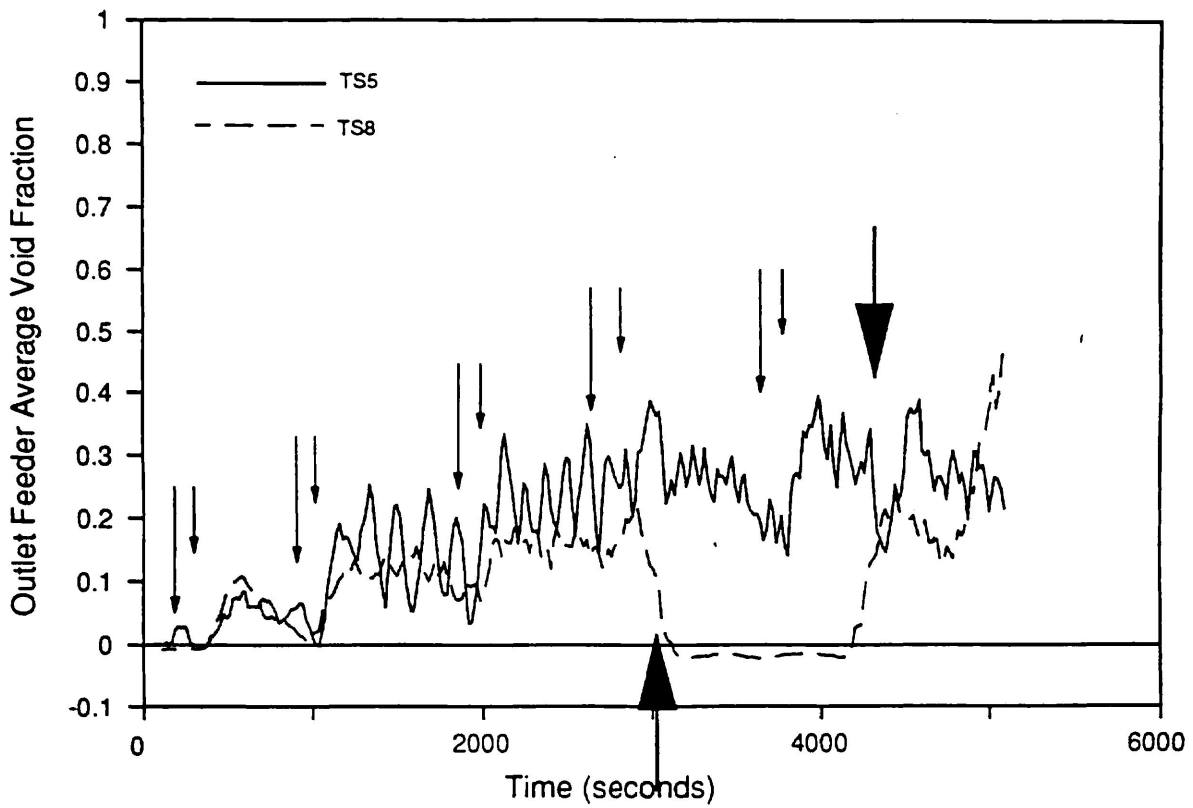


Figure 16. Comparison of Outlet Feeder Average Void Fraction in Channels 5 and 8 in Test T8809.

T8809

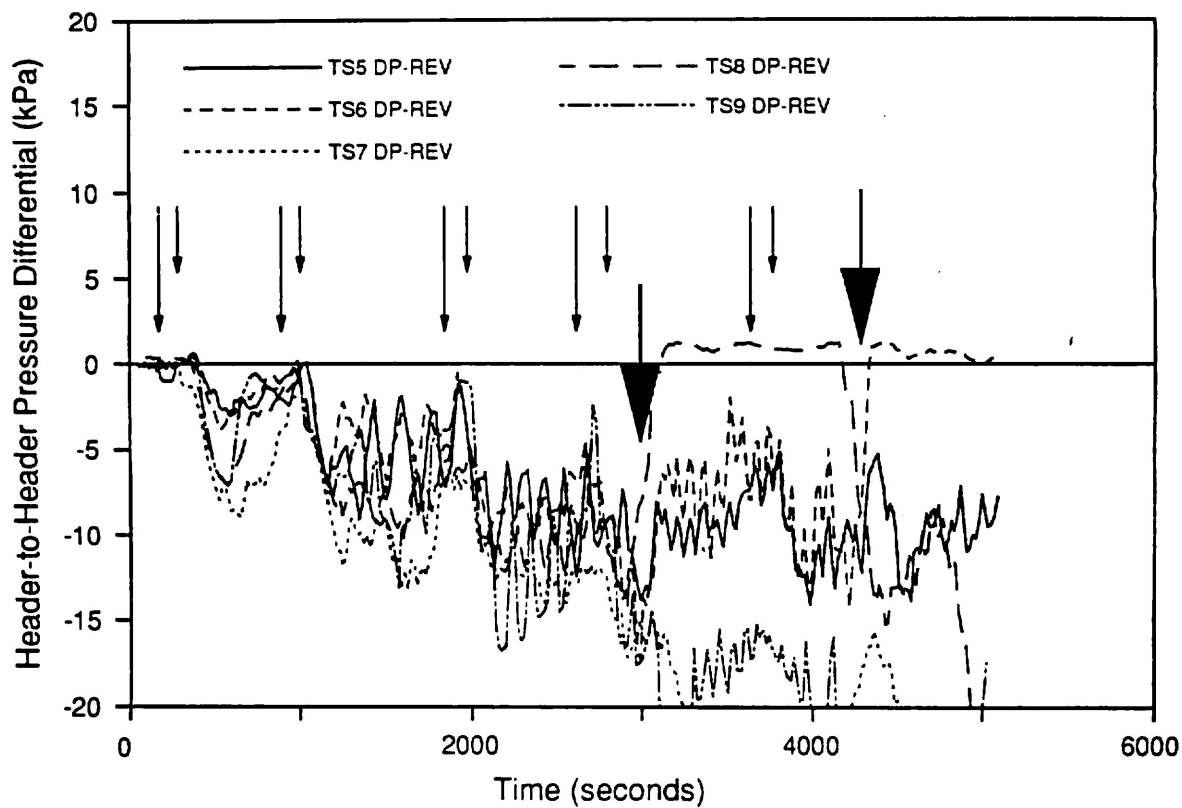


Figure 17. Header-to-Header Pressure Differential Required for Channel Flow Reversal in Channels 5 to 9 as a Function of Time in Test T8809.

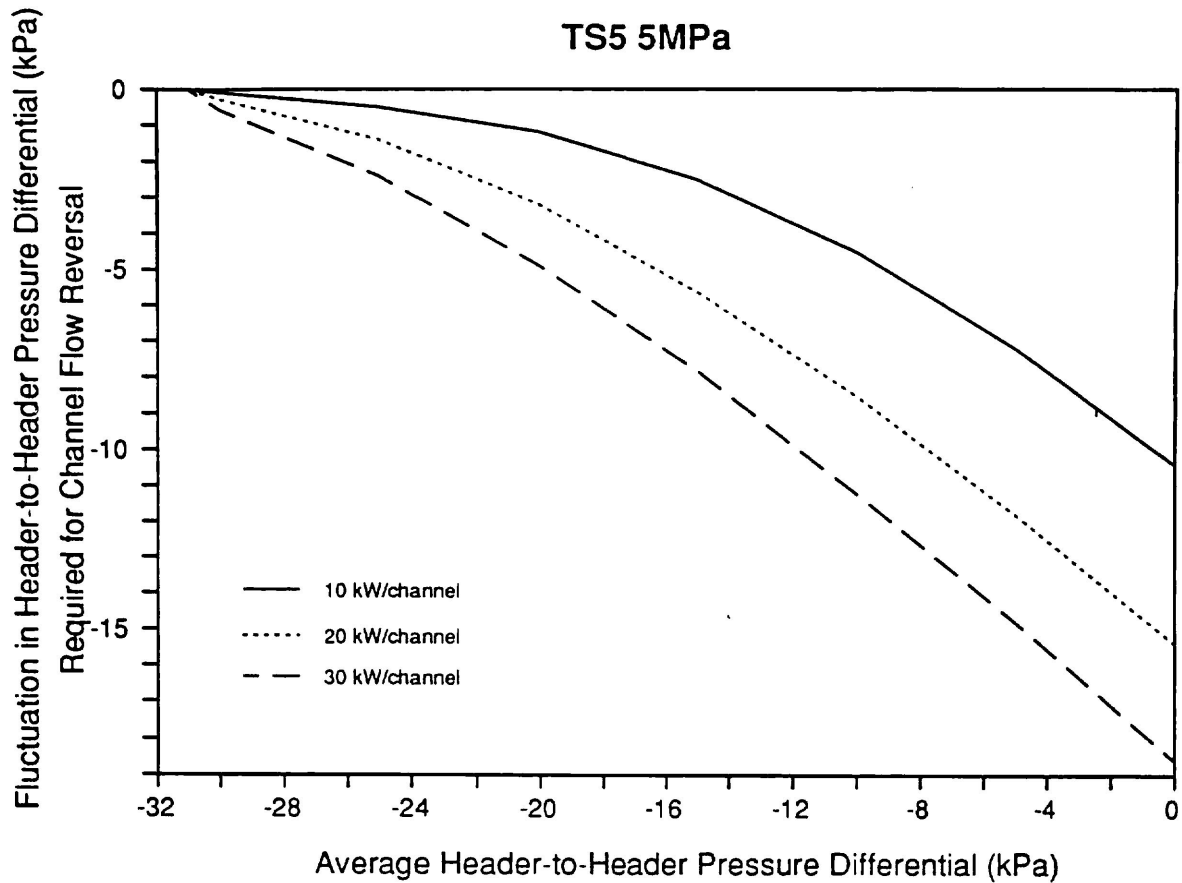


Figure 18. Fluctuation in Header-to-Header Pressure Differential Predicted to Be Required for Reversing Flow in Channel 5 as a Function of the Average Header-to-Header Pressure Differential for Various Channel Powers at 5 MPa Pressure.

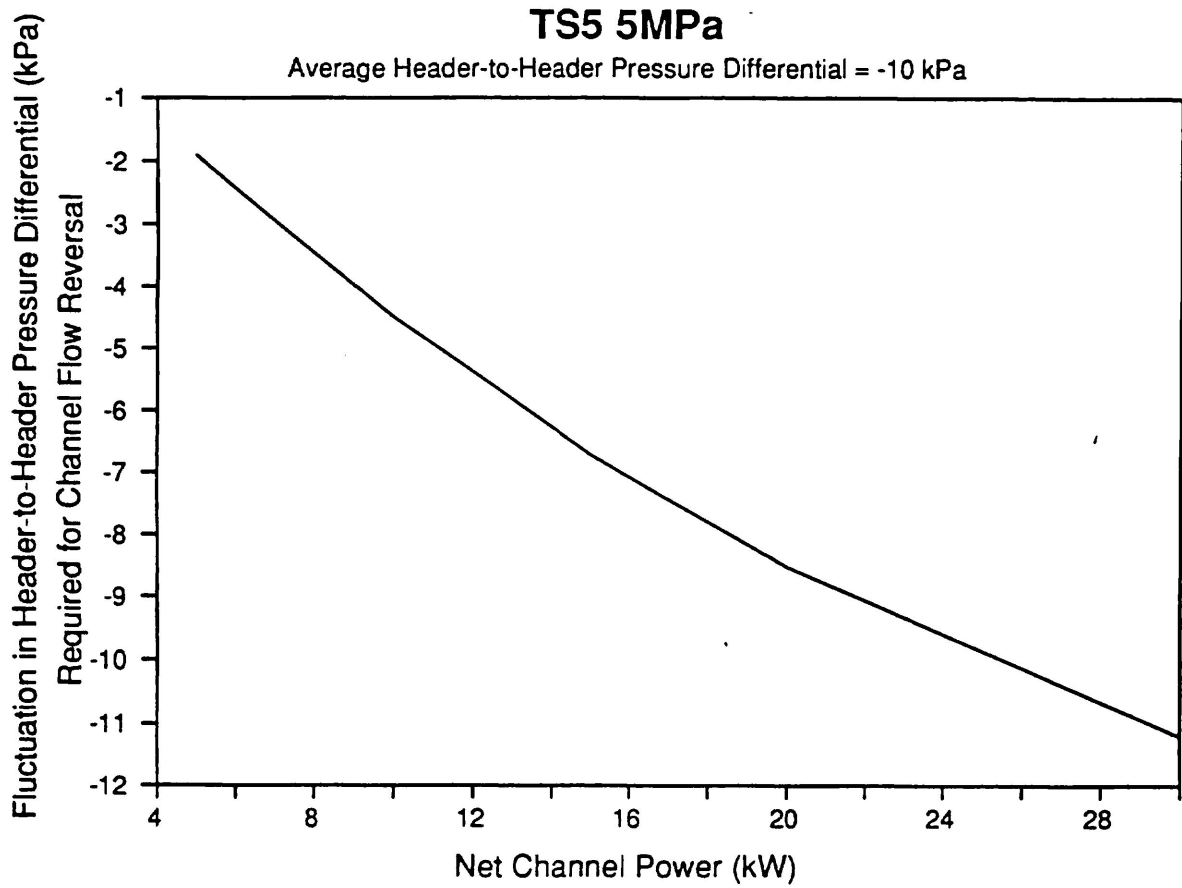


Figure 19. Fluctuation in Header-to-Header Pressure Differential Predicted to Be Required for Reversing Flow in Channel 5 as a Function of the Net Channel Power at an Average Header-to-Header Pressure Differential of -10 kPa and a Pressure of 5 MPa.